Measurement of integrated luminosities at BESIII for data samples at center-of-mass energies between 4.0 and 4.6 GeV

Measurement of integrated luminosities at BESIII for data samples at center-of-mass energies between 4.0 and 4.6 GeV

M. Ablikim[1], M. N. Achasov[10,b], P. Adlarson[68], S. Ahmed[14], M. Albrecht[4], R. Aliberti[28], A. Amoroso[67A,67C], M. R. An[32], Q. An[64,50], X. H. Bai[58], Y. Bai[49], O. Bakina[29], R. Baldini Ferroli[23A], I. Balossino[24A], Y. Ban[39,h], V. Batozskaya[1,37], D. Becker[28], K. Begzsuren[26], N. Berger[28], M. Bertani[23A], D. Bettoni[24A], F. Bianchi[67A,67C], J. Bloms[61], A. Bortone[67A,67C], I. Boyko[29], R. A. Briere[5], H. Cai[69], X. Cai[1,50], A. Calcaterra[23A], G. F. Cao[1,55], N. Cao[1,55], S. A. Cetin[54A], J. F. Chang[1,50], W. L. Chang[1,55], G. Chelkov[29,a], C. Chen[36], G. Chen[1], H. S. Chen[1,55], M. L. Chen[1,50], S. J. Chen[35], T. Chen[1], X. R. Chen[25], X. T. Chen[1], Y. B. Chen[1,50], Z. J. Chen[20,i], W. S. Cheng[67C], G. Cibinetto[24A], F. Cossio[67C], J. J. Cui[42], X. F. Cui[36], H. L. Dai[1,50], J. P. Dai[71], X. C. Dai[1,55], A. Dbeyssi[14], R. E. de Boer[4], D. Dedovich[29], Z. Y. Deng[1], A. Denig[28], I. Denysenko[29], M. Destefanis[67A,67C], F. De Mori[67A,67C], Y. Ding[33], C. Dong[36], J. Dong[1,50], L. Y. Dong[1,55], M. Y. Dong[1,50,55], X. Dong[69], S. X. Du[73], P. Egorov[29,a], Y. L. Fan[69], J. Fang[1,50], S. S. Fang[1,55], Y. Fang[1], R. Farinelli[24A], L. Fava[67B,67C], F. Feldbauer[4], G. Felici[23A], C. Q. Feng[64,50], J. H. Feng[51], M. Fritsch[4], C. D. Fu[1], Y. N. Gao[39,h], Yang Gao[64,50], I. Garzia[24A,24B], P. T. Ge[69], C. Geng[51], E. M. Gersabeck[59], A Gilman[62], K. Goetzen[11], L. Gong[33], W. X. Gong[1,50], W. Gradl[28], M. Greco[67A,67C], M. H. Gu[1,50], C. Y Guan[1,55], A. Q. Guo[22], A. Q. Guo[25], L. B. Guo[34], R. P. Guo[41], Y. P. Guo[9,g], A. Guskov[29,a], T. T. Han[42], W. Y. Han[32], X. Q. Hao[15], F. A. Harris[57], K. K. He[47], K. L. He[1,55], F. H. Heinsius[4], C. H. Heinz[28], Y. K. Heng[1,50,55], C. Herold[52], M. Himmelreich[11,e], T. Holtmann[4], G. Y. Hou[1,55], Y. R. Hou[55], Z. L. Hou[1], H. M. Hu[1,55], J. F. Hu[48,j], T. Hu[1,50,55], Y. Hu[1], G. S. Huang[64,50], L. Q. Huang[65], X. T. Huang[42], Y. P. Huang[1], Z. Huang[39,h], T. Hussain[66], N Hüsken[22,28], W. Ikegami Andersson[68], W. Imoehl[22], M. Irshad[64,50], S. Jaeger[4], S. Janchiv[26], Q. Ji[1], Q. P. Ji[15], X. B. Ji[1,55], X. L. Ji[1,50], Y. Y. Ji[42], H. B. Jiang[42], S. S. Jiang[32], X. S. Jiang[1,50,55], J. B. Jiao[42], Z. Jiao[18], S. Jin[35], Y. Jin[58], M. Q. Jing[1,55], T. Johansson[68], N. Kalantar-Nayestanaki[56], X. S. Kang[33], R. Kappert[56], M. Kavatsyuk[56], B. C. Ke[73], I. K. Keshk[4], A. Khoukaz[61], P. Kiese[28], R. Kiuchi[1], R. Kliemt[11], L. Koch[30], O. B. Kolcu[54A], B. Kopf[4], M. Kuemmel[4], M. Kuessner[4], A. Kupsc[37,68], M. G. Kurth[1,55], W. Kühn[30], J. J. Lane[59], J. S. Lange[30], P. Larin[14], A. Lavania[21], L. Lavezzi[67A,67C], Z. H. Lei[64,50], H. Leithoff[28], M. Lellmann[28], T. Lenz[28], C. Li[40], C. Li[36], C. H. Li[32], Cheng Li[64,50], D. M. Li[73], F. Li[1,50], G. Li[1], H. Li[64,50], H. Li[44], H. B. Li[1,55], H. J. Li[15], H. N. Li[48,j], J. L. Li[42], J. Q. Li[4], J. S. Li[51], Ke Li[1], L. J Li[1], L. K. Li[1], Lei Li[3], M. H. Li[36], P. R. Li[31,k,l], S. X. Li[9], S. Y. Li[53], T. Li[42], W. D. Li[1,55], W. G. Li[1], X. H. Li[64,50], X. L. Li[42], Xiaoyu Li[1,55], Z. Y. Li[51], H. Liang[64,50], H. Liang[27], H. Liang[1,55], Y. F. Liang[46], Y. T. Liang[25], G. R. Liao[12], L. Z. Liao[1,55], J. Libby[21], A. Limphirat[52], C. X. Lin[51], D. X. Lin[25], T. Lin[1], B. J. Liu[1], C. X. Liu[1], D. Liu[14,64], F. H. Liu[45], Fang Liu[1], Feng Liu[6], G. M. Liu[48,j], H. M. Liu[1,55], Huanhuan Liu[1], Huihui Liu[16], J. B. Liu[64,50], J. L. Liu[65], J. Y. Liu[1,55], K. Liu[1], K. Y. Liu[33], Ke Liu[17], L. Liu[64,50], M. H. Liu[9,g], P. L. Liu[1], Q. Liu[55], S. B. Liu[64,50], T. Liu[1,55], T. Liu[9,g], W. M. Liu[64,50], X. Liu[31,k,l], Y. Liu[31,k,l], Y. B. Liu[36], Z. A. Liu[1,50,55], Z. Q. Liu[42], X. C. Lou[1,50,55], F. X. Lu[51], H. J. Lu[18], J. D. Lu[1,55], J. G. Lu[1,50], X. L. Lu[1], Y. Lu[1], Y. P. Lu[1,50], Z. H. Lu[1], C. L. Luo[34], M. X. Luo[72], T. Luo[9,g], X. L. Luo[1,50], X. R. Lyu[55], Y. F. Lyu[36], F. C. Ma[33], H. L. Ma[1], L. L. Ma[42], M. M. Ma[1,55], Q. M. Ma[1], R. Q. Ma[1,55], R. T. Ma[55], X. X. Ma[1,55], X. Y. Ma[1,50], Y. Ma[39,h], F. E. Maas[14], M. Maggiora[67A,67C], S. Maldaner[4], S. Malde[62], Q. A. Malik[66], A. Mangoni[23B], Y. J. Mao[39,h], Z. P. Mao[1], S. Marcello[67A,67C], Z. X. Meng[58], J. G. Messchendorp[56,d], G. Mezzadri[24A], H. Miao[1], T. J. Min[35], R. E. Mitchell[22], X. H. Mo[1,50,55], N. Yu. Muchnoi[10,b], H. Muramatsu[60], S. Nakhoul[11,e], Y. Nefedov[29], F. Nerling[11,e], I. B. Nikolaev[10,b], Z. Ning[1,50], S. Nisar[8,m], S. L. Olsen[55], Q. Ouyang[1,50,55], S. Pacetti[23B,23C], X. Pan[9,g], Y. Pan[59], A. Pathak[1], A. Pathak[27], P. Patteri[23A], M. Pelizaeus[4], H. P. Peng[64,50], K. Peters[11,e], J. Pettersson[68],

J. L. Ping[34], R. G. Ping[1,55], S. Plura[28], S. Pogodin[29], R. Poling[60], V. Prasad[64,50], H. Qi[64,50], H. R. Qi[53], M. Qi[35], T. Y. Qi[9,g], S. Qian[1,50], W. B. Qian[55], Z. Qian[51], C. F. Qiao[55], J. J. Qin[65], L. Q. Qin[12], X. P. Qin[9,g], X. S. Qin[42], Z. H. Qin[1,50], J. F. Qiu[1], S. Q. Qu[36], K. H. Rashid[66], K. Ravindran[21], C. F. Redmer[28], K. J. Ren[32], A. Rivetti[67C], V. Rodin[56], M. Rolo[67C], G. Rong[1,55], Ch. Rosner[14], M. Rump[61], H. S. Sang[64], A. Sarantsev[29,c], Y. Schelhaas[28], C. Schnier[4], K. Schoenning[68], M. Scodeggio[24A,24B], K. Y. Shan[9,g], W. Shan[19], X. Y. Shan[64,50], J. F. Shangguan[47], L. G. Shao[1,55], M. Shao[64,50], C. P. Shen[9,g], H. F. Shen[1,55], X. Y. Shen[1,55], B.-A. Shi[55], H. C. Shi[64,50], R. S. Shi[1,55], X. Shi[1,50], X. D Shi[64,50], J. J. Song[15], W. M. Song[27,1], Y. X. Song[39,h], S. Sosio[67A,67C], S. Spataro[67A,67C], F. Stieler[28], K. X. Su[69], P. P. Su[47], Y.-J. Su[55], G. X. Sun[1], H. K. Sun[1], J. F. Sun[15], L. Sun[69], S. S. Sun[1,55], T. Sun[1,55], W. Y. Sun[27], X Sun[20,i], Y. J. Sun[64,50], Y. Z. Sun[1], Z. T. Sun[42], Y. H. Tan[69], Y. X. Tan[64,50], C. J. Tang[46], G. Y. Tang[1], J. Tang[51], L. Y Tao[65], Q. T. Tao[20,i], J. X. Teng[64,50], V. Thoren[68], W. H. Tian[44], Y. T. Tian[25], I. Uman[54B], B. Wang[1], D. Y. Wang[39,h], F. Wang[65], H. J. Wang[31,k,l], H. P. Wang[1,55], K. Wang[1,50], L. L. Wang[1], M. Wang[42], M. Z. Wang[39,h], Meng Wang[1,55], S. Wang[9,g], T. J. Wang[36], W. Wang[51], W. H. Wang[69], W. P. Wang[64,50], X. Wang[39,h], X. F. Wang[31,k,l], X. L. Wang[9,g], Y. D. Wang[38], Y. F. Wang[1,50,55], Y. Q. Wang[1], Y. Y. Wang[31,k,l], Ying Wang[51], Z. Wang[1,50], Z. Y. Wang[1], Ziyi Wang[55], Zongyuan Wang[1,55], D. H. Wei[12], F. Weidner[61], S. P. Wen[1], D. J. White[59], U. Wiedner[4], G. Wilkinson[62], M. Wolke[68], L. Wollenberg[4], J. F. Wu[1,55], L. H. Wu[1], L. J. Wu[1,55], X. Wu[9,g], X. H. Wu[27], Z. Wu[1,50], L. Xia[64,50], T. Xiang[39,h], H. Xiao[9,g], S. Y. Xiao[1], Y. L. Xiao[9,g], Z. J. Xiao[34], X. H. Xie[39,h], Y. G. Xie[1,50], Y. H. Xie[6], T. Y. Xing[1,55], C. F. Xu[1], C. J. Xu[51], G. F. Xu[1], Q. J. Xu[13], W. Xu[1,55], X. P. Xu[47], Y. C. Xu[55], F. Yan[9,g], L. Yan[9,g], W. B. Yan[64,50], W. C. Yan[73], H. J. Yang[43,f], H. X. Yang[1], L. Yang[44], S. L. Yang[55], Y. X. Yang[1,55], Y. X. Yang[12], Yifan Yang[1,55], Zhi Yang[25], M. Ye[1,50], M. H. Ye[7], J. H. Yin[1], Z. Y. You[51], B. X. Yu[1,50,55], C. X. Yu[36], G. Yu[1,55], J. S. Yu[20,i], T. Yu[65], C. Z. Yuan[1,55], L. Yuan[2], S. C. Yuan[1], X. Q. Yuan[1], Y. Yuan[1], Z. Y. Yuan[51], C. X. Yue[32], A. A. Zafar[66], X. Zeng Zeng[6], Y. Zeng[20,i], A. Q. Zhang[1], B. L. Zhang[1], B. X. Zhang[1], G. Y. Zhang[15], H. Zhang[64], H. H. Zhang[51], H. H. Zhang[27], H. Y. Zhang[1,50], J. L. Zhang[70], J. Q. Zhang[34], J. W. Zhang[1,50,55], J. Y. Zhang[1], J. Z. Zhang[1,55], Jianyu Zhang[1,55], Jiawei Zhang[1,55], L. M. Zhang[53], L. Q. Zhang[51], Lei Zhang[35], P. Zhang[1], Shulei Zhang[20,i], X. D. Zhang[38], X. M. Zhang[1], X. Y. Zhang[47], X. Y. Zhang[42], Y. Zhang[62], Y. T. Zhang[73], Y. H. Zhang[1,50], Yan Zhang[64,50], Yao Zhang[1], Z. H. Zhang[1], Z. Y. Zhang[69], Z. Y. Zhang[36], G. Zhao[1], J. Zhao[32], J. Y. Zhao[1,55], J. Z. Zhao[1,50], Lei Zhao[64,50], Ling Zhao[1], M. G. Zhao[36], Q. Zhao[1], S. J. Zhao[73], Y. B. Zhao[1,50], Y. X. Zhao[25], Z. G. Zhao[64,50], A. Zhemchugov[29,a], B. Zheng[65], J. P. Zheng[1,50], Y. H. Zheng[55], B. Zhong[34], C. Zhong[65], L. P. Zhou[1,55], Q. Zhou[1,55], X. Zhou[69], X. K. Zhou[55], X. R. Zhou[64,50], X. Y. Zhou[32], Y. Z. Zhou[9,g], A. N. Zhu[1,55], J. Zhu[36], K. Zhu[1], K. J. Zhu[1,50,55], S. H. Zhu[63], T. J. Zhu[70], W. J. Zhu[36], W. J. Zhu[9,g], Y. C. Zhu[64,50], Z. A. Zhu[1,55], B. S. Zou[1], J. H. Zou[1], Y. T. Gu[74], H. B. Liu[74]

(BESIII Collaboration)

[1] *Institute of High Energy Physics, Beijing 100049, People's Republic of China*

[2] *Beihang University, Beijing 100191, People's Republic of China*

[3] *Beijing Institute of Petrochemical Technology, Beijing 102617, People's Republic of China*

[4] *Bochum Ruhr-University, D-44780 Bochum, Germany*

[5] *Carnegie Mellon University, Pittsburgh, Pennsylvania 15213, USA*

[6] *Central China Normal University, Wuhan 430079, People's Republic of China*

[7] *China Center of Advanced Science and Technology, Beijing 100190, People's Republic of China*

[8] *COMSATS University Islamabad, Lahore Campus, Defence Road, Off Raiwind Road, 54000 Lahore, Pakistan*

[9] *Fudan University, Shanghai 200443, People's Republic of China*

[10] *G.I. Budker Institute of Nuclear Physics SB RAS (BINP), Novosibirsk 630090, Russia*
[11] *GSI Helmholtzcentre for Heavy Ion Research GmbH, D-64291 Darmstadt, Germany*
[12] *Guangxi Normal University, Guilin 541004, People's Republic of China*
[13] *Hangzhou Normal University, Hangzhou 310036, People's Republic of China*
[14] *Helmholtz Institute Mainz, Staudinger Weg 18, D-55099 Mainz, Germany*
[15] *Henan Normal University, Xinxiang 453007, People's Republic of China*
[16] *Henan University of Science and Technology, Luoyang 471003, People's Republic of China*
[17] *Henan University of Technology, Zhengzhou 450001, People's Republic of China*
[18] *Huangshan College, Huangshan 245000, People's Republic of China*
[19] *Hunan Normal University, Changsha 410081, People's Republic of China*
[20] *Hunan University, Changsha 410082, People's Republic of China*
[21] *Indian Institute of Technology Madras, Chennai 600036, India*
[22] *Indiana University, Bloomington, Indiana 47405, USA*
[23] *INFN Laboratori Nazionali di Frascati , (A)INFN Laboratori Nazionali di Frascati, I-00044, Frascati, Italy; (B)INFN Sezione di Perugia, I-06100, Perugia, Italy; (C)University of Perugia, I-06100, Perugia, Italy*
[24] *INFN Sezione di Ferrara, (A)INFN Sezione di Ferrara, I-44122, Ferrara, Italy; (B)University of Ferrara, I-44122, Ferrara, Italy*
[25] *Institute of Modern Physics, Lanzhou 730000, People's Republic of China*
[26] *Institute of Physics and Technology, Peace Ave. 54B, Ulaanbaatar 13330, Mongolia*
[27] *Jilin University, Changchun 130012, People's Republic of China*
[28] *Johannes Gutenberg University of Mainz, Johann-Joachim-Becher-Weg 45, D-55099 Mainz, Germany*
[29] *Joint Institute for Nuclear Research, 141980 Dubna, Moscow region, Russia*
[30] *Justus-Liebig-Universitaet Giessen, II. Physikalisches Institut, Heinrich-Buff-Ring 16, D-35392 Giessen, Germany*
[31] *Lanzhou University, Lanzhou 730000, People's Republic of China*
[32] *Liaoning Normal University, Dalian 116029, People's Republic of China*
[33] *Liaoning University, Shenyang 110036, People's Republic of China*
[34] *Nanjing Normal University, Nanjing 210023, People's Republic of China*
[35] *Nanjing University, Nanjing 210093, People's Republic of China*
[36] *Nankai University, Tianjin 300071, People's Republic of China*
[37] *National Centre for Nuclear Research, Warsaw 02-093, Poland*
[38] *North China Electric Power University, Beijing 102206, People's Republic of China*
[39] *Peking University, Beijing 100871, People's Republic of China*
[40] *Qufu Normal University, Qufu 273165, People's Republic of China*
[41] *Shandong Normal University, Jinan 250014, People's Republic of China*
[42] *Shandong University, Jinan 250100, People's Republic of China*
[43] *Shanghai Jiao Tong University, Shanghai 200240, People's Republic of China*
[44] *Shanxi Normal University, Linfen 041004, People's Republic of China*
[45] *Shanxi University, Taiyuan 030006, People's Republic of China*
[46] *Sichuan University, Chengdu 610064, People's Republic of China*
[47] *Soochow University, Suzhou 215006, People's Republic of China*
[48] *South China Normal University, Guangzhou 510006, People's Republic of China*
[49] *Southeast University, Nanjing 211100, People's Republic of China*
[50] *State Key Laboratory of Particle Detection and Electronics, Beijing 100049, Hefei 230026, People's Republic of China*

[51] Sun Yat-Sen University, Guangzhou 510275, People's Republic of China
[52] Suranaree University of Technology, University Avenue 111, Nakhon Ratchasima 30000, Thailand
[53] Tsinghua University, Beijing 100084, People's Republic of China
[54] Turkish Accelerator Center Particle Factory Group, (A)Istinye University, 34010, Istanbul, Turkey; (B)Near East University, Nicosia, North Cyprus, Mersin 10, Turkey
[55] University of Chinese Academy of Sciences, Beijing 100049, People's Republic of China
[56] University of Groningen, NL-9747 AA Groningen, The Netherlands
[57] University of Hawaii, Honolulu, Hawaii 96822, USA
[58] University of Jinan, Jinan 250022, People's Republic of China
[59] University of Manchester, Oxford Road, Manchester, M13 9PL, United Kingdom
[60] University of Minnesota, Minneapolis, Minnesota 55455, USA
[61] University of Muenster, Wilhelm-Klemm-Str. 9, 48149 Muenster, Germany
[62] University of Oxford, Keble Rd, Oxford, UK OX13RH
[63] University of Science and Technology Liaoning, Anshan 114051, People's Republic of China
[64] University of Science and Technology of China, Hefei 230026, People's Republic of China
[65] University of South China, Hengyang 421001, People's Republic of China
[66] University of the Punjab, Lahore-54590, Pakistan
[67] University of Turin and INFN, (A)University of Turin, I-10125, Turin, Italy; (B)University of Eastern Piedmont, I-15121, Alessandria, Italy; (C)INFN, I-10125, Turin, Italy
[68] Uppsala University, Box 516, SE-75120 Uppsala, Sweden
[69] Wuhan University, Wuhan 430072, People's Republic of China
[70] Xinyang Normal University, Xinyang 464000, People's Republic of China
[71] Yunnan University, Kunming 650500, People's Republic of China
[72] Zhejiang University, Hangzhou 310027, People's Republic of China
[73] Zhengzhou University, Zhengzhou 450001, People's Republic of China
[74] Guangxi University, Nanning 530004, People's Republic of China

[a] Also at the Moscow Institute of Physics and Technology, Moscow 141700, Russia
[b] Also at the Novosibirsk State University, Novosibirsk, 630090, Russia
[c] Also at the NRC "Kurchatov Institute", PNPI, 188300, Gatchina, Russia
[d] Currently at Istanbul Arel University, 34295 Istanbul, Turkey
[e] Also at Goethe University Frankfurt, 60323 Frankfurt am Main, Germany
[f] Also at Key Laboratory for Particle Physics, Astrophysics and Cosmology, Ministry of Education; Shanghai Key Laboratory for Particle Physics and Cosmology; Institute of Nuclear and Particle Physics, Shanghai 200240, People's Republic of China
[g] Also at Key Laboratory of Nuclear Physics and Ion-beam Application (MOE) and Institute of Modern Physics, Fudan University, Shanghai 200443, People's Republic of China
[h] Also at State Key Laboratory of Nuclear Physics and Technology, Peking University, Beijing 100871, People's Republic of China
[i] Also at School of Physics and Electronics, Hunan University, Changsha 410082, China
[j] Also at Guangdong Provincial Key Laboratory of Nuclear Science, Institute of Quantum Matter, South China Normal University, Guangzhou 510006, China
[k] Also at Frontiers Science Center for Rare Isotopes, Lanzhou University, Lanzhou 730000, People's Republic of China
[l] Also at Lanzhou Center for Theoretical Physics, Lanzhou University, Lanzhou 730000, People's Republic of China

[m] *Also at the Department of Mathematical Sciences, IBA, Karachi , Pakistan*

(Dated: November 29, 2022)

Abstract

The integrated luminosities of the data samples collected in the BESIII experiment in 2016–2017 at center-of-mass energies between 4.19 and 4.28 GeV are measured with a precision better than 1% by analyzing large-angle Bhabha scattering events. The integrated luminosities of the old data sets collected in 2010–2014 are updated by considering correction related to the detector performance, offsettting the effect of newly discovered readout errors in the electromagnetic calorimeter that happen haphazardly.

Keywords: Integrated luminosity, e^+e^- annihilation, Bhabha scattering

I. INTRODUCTION

In recent years, the newly discovered charmonium-like states have drawn great attention due to their exotic properties [4]. These states are above the open-charm threshold, and their strong coupling to hidden-charm processes suggests that they could be candidates for unconventional charmonium states. Study of the properties of these states, through either verifying or excluding possible interpretations about their exotic nature (such as molecular states, tetraquark states, hybrid states, etc.), or establishing the connection between these states and higher excited charmonium states, has the potential to provide more insight into the quark model and a better understanding of quantum chromodynamics (QCD).

The BESIII experiment [1], which operates at the τ-charm factory BEPCII [2], has collected the world's largest e^+e^- collision data samples at center-of-mass (CM) energies between 3.81 and 4.60 GeV [3]. In this energy region, the charmonium-like states (also called XYZ states), together with higher excited charmonium states, can be produced copiously, and comprehensive studies of these particles can be performed. Also, the data can be used in other studies beyond the field of charmonium physics, such as R measurement or on various topics in charm physics.

To shed light on the topics mentioned above, it is essential to measure the production cross sections of these states, which in return require the precise knowledge of the time-integrated luminosities of the relevant data samples.

In this paper, we present the results of the luminosity measurements for the XYZ data samples taken by BESIII from December 2016 to May 2017, as well as an update on the previous measurement for the XYZ data samples taken from December 2011 to May 2014 [5]. The update is necessary since a malfunction of the detector that was not modelled in Monte Carlo (MC) simulation, which resulted in an underestimation of the previously measured integrated luminosities, has been recently discovered. The measurement is based on analysis of the Bhabha scattering process $e^+e^- \to (\gamma)e^+e^-$, and the procedure we take is similar to the one in a previous BESIII analysis [5]. The process is chosen for its clean signature and large production cross section, which is known with high theoretical precision. These features allow a precise measurement with small statistical and systematic uncertainties.

II. THE BESIII DETECTOR AND DATA SAMPLES

BESIII is a general purpose detector which operates at the e^+e^- collider BEPCII [2]. Due to the crossing angle of the beams at the interaction point, the e^+e^- CM system is slightly boosted

with respect to the laboratory frame. A detailed description of the facility is given in Ref. [1]. The cylindrical core of the BESIII detector covers 93% of the full solid angle and consists of a helium-based multilayer drift chamber (MDC), a plastic scintillator time-of-flight system (TOF), and a CsI(Tl) electromagnetic calorimeter (EMC), which are all enclosed in a superconducting solenoidal magnet providing a 1.0 T magnetic field. The solenoid is supported by an octagonal flux-return yoke with resistive plate counter muon identification modules interleaved with steel. The charged-particle momentum resolution at $1\ \mathrm{GeV}/c$ is 0.5%, and the dE/dx resolution is 6% for electrons from Bhabha scattering. The EMC measures photon energies with a resolution of 2.5% (5%) at 1 GeV in the barrel (end-cap) region. The time resolution in the TOF barrel region is 68 ps, whereas that in the end-cap region is 110 ps. The end-cap TOF system was upgraded in 2015 using multi-gap resistive plate chamber technology, providing a time resolution of 60 ps [6]. A GEANT4 [7] based detector simulation package has been developed to model the detector response.

From December 2016 to May 2017, eight data sets were taken at CM energies between 4.19 and 4.28 GeV. These data sets were collected in the vicinity of the $Y(4230)$ and $Y(4320)$ resonances, aimed at studying the line shapes of the production cross sections and the decay properties of these charmonium-like states. The CM energy ($E_{\rm CM}$) of each data sample has been determined with the process $e^+e^- \to \mu^+\mu^-$ [8], and is listed in Table I.

TABLE I. Summary of the integrated luminosity results for the 2016–2017 XYZ data samples. $N_{\rm cor}$ is the number of events recovered by the correction for the EMC readout error as defined in Section IV. The first uncertainties are statistical and the second ones are systematic.

Sample	$E_{\rm CM}$ (MeV)	$N_{\rm obs}$ ($\times 10^6$)	$N_{\rm cor}$ ($\times 10^6$)	σ_{Bhabha} (nb)	ε (%)	$\mathcal{L}$ (pb^{-1})
4190	4189.12	32.62	0.04	354.82	17.60	526.7$\pm$0.1 $\pm$ 2.2
4200	4199.15	32.59	0.05	353.88	17.53	526.0$\pm$0.1 $\pm$ 2.1
4210	4209.39	31.73	0.05	352.98	17.40	517.1$\pm$0.1 $\pm$ 1.8
4220	4218.93	31.45	0.05	352.42	17.41	514.6$\pm$0.1 $\pm$ 1.8
4237	4235.77	32.32	0.07	350.79	17.41	530.3$\pm$0.1 $\pm$ 2.7
4246	4243.97	32.65	0.07	350.26	17.38	538.1$\pm$0.1 $\pm$ 2.6
4270	4266.81	31.86	0.08	348.01	17.31	531.1$\pm$0.1 $\pm$ 3.1
4280	4277.78	10.46	0.03	346.92	17.21	175.7$\pm$0.1 $\pm$ 1.0

For each data set, two million Bhabha events were generated with the BABAYAGA@NLO [9] generator, using the parameters presented in Table II. In the simulation, the scattering polar angle of the final state electrons has been limited to a range from 20° ($\theta_{\rm min}$) to 160° ($\theta_{\rm max}$), fully covering the detector acceptance. The beam energy is set to the value determined with $e^+e^- \to \mu^+\mu^-$ events in the same data set [8], and the energy spread is set to be 1.364 MeV. An energy threshold of 1.0 GeV ($E_{\rm min}$) is applied to the final-state electrons and positrons. The acollinearity of the events (i.e. the angle between the electron and the reverse extension line of the positron) and the number of photons from initial/final state radiation are not constrained. Additionally, a selection on the invariant mass of the e^+e^- pair ($M(e^+e^-)$) larger than 3.8 GeV/c^2 has been applied, to reduce the computing time for simulation by avoiding the need to sample over narrow states such as the $\psi(2S)$ and J/ψ resonances.

TABLE II. Parameters of the BABAYAGA@NLO generator for MC sample at $E_{\rm CM} = 4.19$ GeV. For the other energy points, only the $E_{\rm CM}$ setting changes.

Parameter	Value
$E_{\rm CM}$ (MeV)	4189.12
Beam Energy Spread (MeV)	1.364
$\theta_{\rm min}$ ($^\circ$)	20
$\theta_{\rm max}$ ($^\circ$)	160
Maximum Acollinearity ($^\circ$)	180
$E_{\rm min}$ (GeV)	1
$M(e^+e^-)$ (GeV/c^2)	> 3.8

III. EVENT SELECTION

Signal Bhabha candidate events are required to have two oppositely charged good tracks. The good tracks must originate from a cylindrical volume, centered around the interaction point, with a radius of 1 cm perpendicular to the beam axis and a length of ± 10 cm along the beam axis. The polar angle of the tracks $\theta_{\rm MDC}$, measured by the MDC and boosted to the e^+e^- CM frame, is required to be in the fiducial volume of $|\cos\theta_{\rm MDC}| < 0.8$. The deposited energy of each track in EMC must be larger than $0.37 \times E_{\rm CM}$, and the momentum of each track has to be larger than $0.47 \times E_{\rm CM}$, to reduce background from di-muon pairs or from the decays of light resonances, respectively. The invariant mass of the track pair is required to be larger than 3.85 GeV/c^2, because only the events with an invariant mass above 3.8 GeV/c^2 are produced in the MC event generator. As demonstrated by a similar previous analysis [5], the remaining background contribution after applying these selection criteria is negligible.

Figure 1 shows the comparison between data and MC simulation for the kinematic variables previously discussed. There is a reasonable agreement in the distributions of all the variables.

IV. EMC READOUT CORRECTION AND LUMINOSITY RESULTS

The energy deposition in the EMC is used to identify the final state electron/positron tracks. In a study of high energy EMC showers we found that the EMC electronics occasionally failed to provide valid signals for crystals with high deposited energy. The problem mainly occurs for the channels in the absolute polar angle ($\cos\theta$) ranges of (0.6, 0.8) close to the horizontal plane. To illustrate this issue, consider the left plot of Fig. 2, which shows the EMC energy deposition of a typical high energy (around 2 GeV) electron or positron shower, where no problem occurs. The shower extends across 5×5 crystals and the deposited energy in crystal numbered (24, 2) is 1592 MeV, one order of magnitude larger than those of the nearby crystals. In contrast, the right plot of Fig. 2 shows an example of a shower missing the readout of the EMC energy deposition from one crystal. Here, the largest energy deposition is expected to be found in the crystal numbered (59, 3) but no valid value is recorded, which leads to an underestimation of the total deposited energy by more than 1 GeV. This effect is not simulated in the MC samples, and must be corrected.

While the reason of this problem is still under investigation, the amount of affected events can be estimated by searching for the MDC tracks with unexpected EMC information. Figure 3 shows

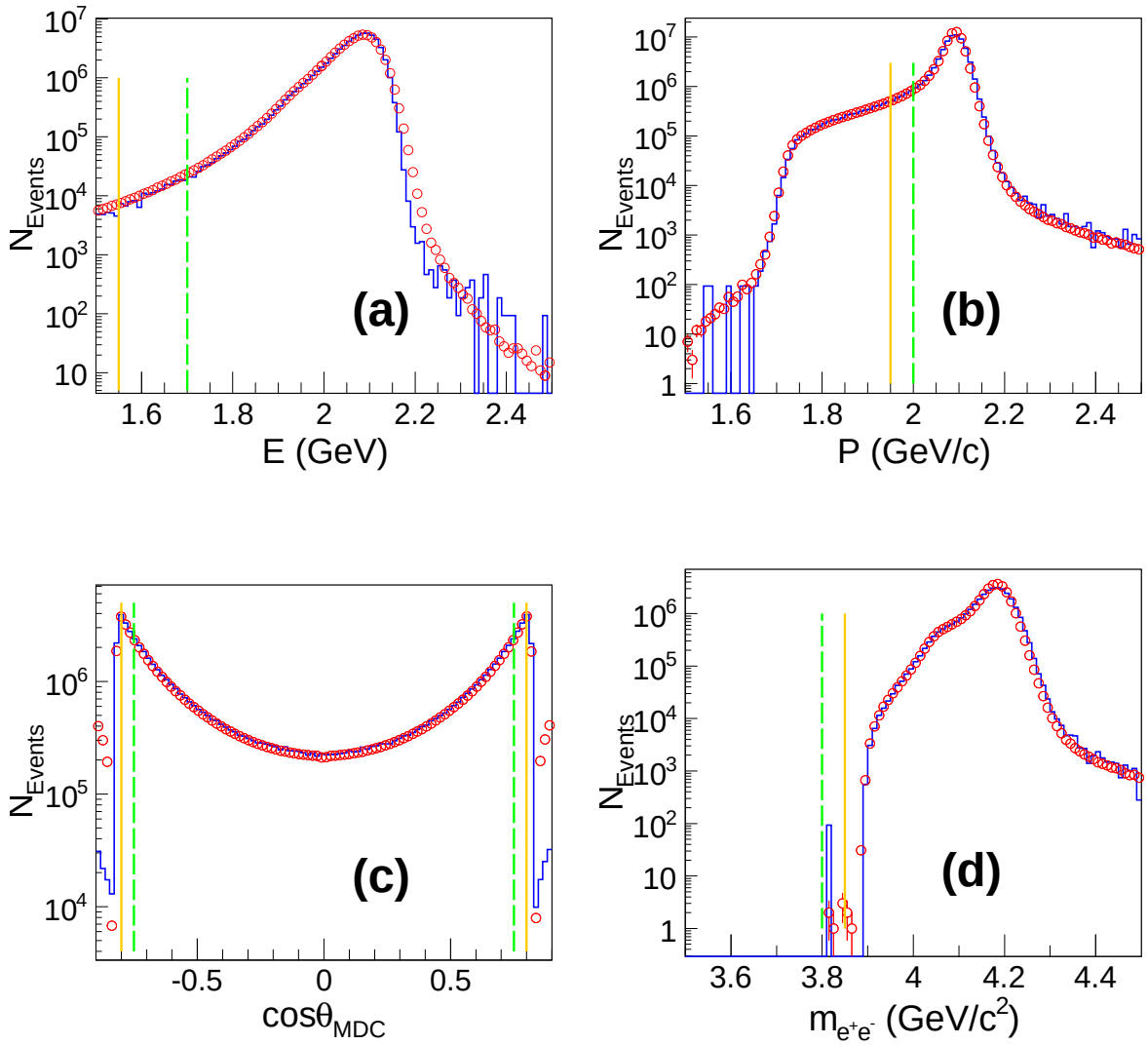

FIG. 1. Data and MC simulation comparison for the variables used in the event selection for the 4190 data sample, including the energy deposition in EMC (a), the momentum (b) and the θ polar angle (c) of electrons and positrons, as well as the invariant mass of the e^+e^- pair (d). Red circles indicate data, while the blue histograms are the MC distributions. Yellow solid lines mark the thresholds for the standard selection criteria, while the green dashed lines indicate altered values used for systematic uncertainty estimation. All the relevant tracks are boosted to the e^+e^- CM frame.

the dielectron deposited energies for events satisfying all the other requirements of our selection criteria, for the MC sample and the experimental data. As one can see in the plots, two abnormal peaks can be found in the data samples, which are not present in the MC sample. These peaks are formed by events where the reconstructed energy deposition by the charged track in the EMC is missing the readout signal from one crystal. To select these events, we apply all the requirements apart from that on the deposited energy in EMC; afterwards, we require that the deposited energy in EMC must be larger than $0.37 \times E_{\rm CM}$ for one track and lower than $0.15 \times E_{\rm CM}$ for the other. The events in which both tracks are affected by EMC readout errors are rare, and their contribution is

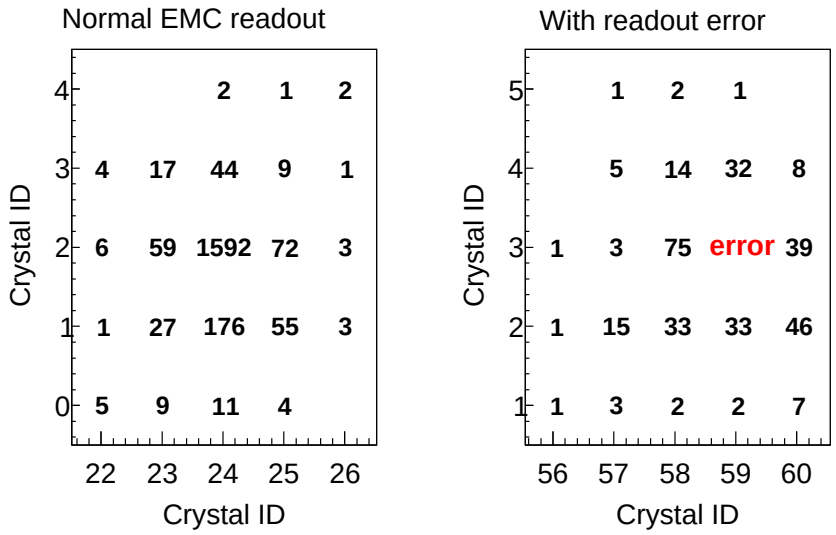

FIG. 2. The EMC energy distributions of a normal EMC shower (left) and an abnormal one suffering from EMC readout errors (right). The x-axis and y-axis mark the EMC crystal ID. The number in each bin represents the deposited energy in the crystal (in MeV). The hitmap of the abnormal track is characterized by a missing value in the middle where major energy deposition is expected.

considered as negligible. Finally, we require that the ionization energy loss of both tracks in MDC must be close to the expected energy loss of electron tracks of the same energy.

Since no normal physics events should be able to pass the above selection, we assume that all the candidates passing the requirements are Bhabha events that suffered from the EMC readout errors. These events are simply added to the sample of observed Bhabha events whose selection is summarized in Section III.

The integrated luminosity is calculated with the equation

$$\mathcal{L} = \frac{N_{\rm obs} + N_{\rm cor}}{\sigma_{\rm Bhabha} \times \varepsilon}, \tag{1}$$

where $N_{\rm obs}$ is the number of observed Bhabha events, $N_{\rm cor}$ is the number of events recovered by the correction of the EMC readout error, $\sigma_{\rm Bhabha}$ is the cross section of the Bhabha process, and ε is the efficiency determined with the signal MC sample. The cross sections are calculated by BABAYAGA@NLO generator using the parameters listed in Table II. All the input numbers and the luminosity results are listed in Table I.

V. SYSTEMATIC UNCERTAINTIES

The following sources of systematic uncertainties are considered: the tracking efficiency, the requirements on the kinematic variables, the limited sizes of the MC samples, the beam energy measurement, the EMC readout correction, and the MC generator.

To estimate the systematic uncertainty of the tracking efficiency, we employed an alternative selection criterion using information from the EMC only. Here, at least two clusters in the EMC

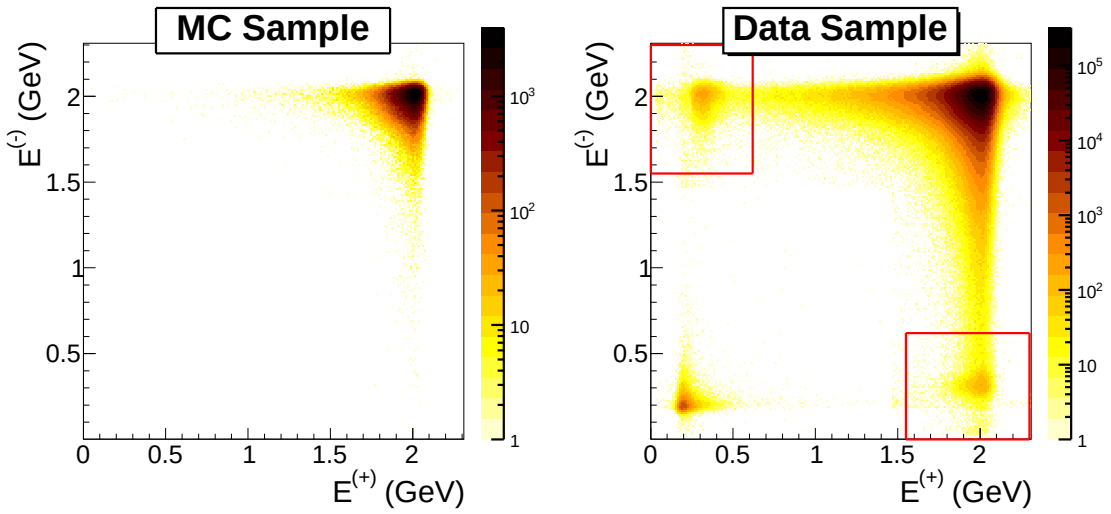

FIG. 3. Deposited energies of positively charged tracks ($E^{(+)}$) and negatively charged tracks ($E^{(-)}$) for the events satisfying all requirements except for the EMC energy depositions, for MC sample (left) and data sample (right) at 4.19 GeV. There are large differences between the energy distributions of the two samples. In the data sample, aside from di-muon events in which the deposited energies of both tracks are low, there are also abnormal events where only one track has low energy deposition (marked by red boxes).

are required; if more than two clusters are present, then the most energetic two are identified as the e^+e^- pair. The deposited energies of the two clusters are required to be larger than $0.45\times E_{\rm CM}$. The polar angle of each cluster is required to satisfy $|\cos\theta_{\rm EMC}| < 0.8$. Additionally, $\Delta\phi$ is required to be in the range of $[-40^\circ,\ -5^\circ]$ or $[5^\circ,\ 40^\circ]$, where $\Delta\phi = |\phi_1 - \phi_2| - 180^\circ$ and $\phi_{1,2}$ are the azimuthal angles of the clusters in the EMC. All the angles are boosted to the e^+e^- CM frame. The difference between the luminosity obtained through this selection and the original result before the EMC readout correction is taken as the systematic uncertainty arising from tracking efficiency.

The systematic uncertainties related to the requirements on the kinematic variables are evaluated by varying the thresholds on the variables. For the requirement on the EMC energy, the alternative threshold is $0.41 \times E_{\rm CM}$; for the polar angle, the alternative range is $[-0.75,\ 0.75]$; for the requirement on momentum, the threshold is changed to $0.48 \times E_{\rm CM}$. For the invariant mass of the e^+e^- pair, the alternative threshold is 3.80 GeV/c^2, and the corresponding uncertainty is found to be negligible.

The statistical uncertainties of the MC samples size, each one having two million events with a selection efficiency of around 17%, are estimated to be 0.2% at each energy point.

The uncertainty on the CM energy measurement is ± 0.6 MeV [8]; its effect on the luminosity determination is estimated by repeating the analysis on the same data sets, while changing the CM energy value by plus and minus this value. To avoid an additional systematical uncertainty due to the MC data sample size, we obtain the detection efficiency and cross section values through the linear extrapolation from the nearby energy points. The uncertainty is estimated as the difference in integrated luminosity compared to our standard result. The small difference between the measured beam-energy spread [10] and that used in the generation of the MC samples leads to a negligible bias in the analysis.

The systematic uncertainty from the EMC readout correction is estimated by comparing the

results with an alternative correcting method, where the events with one or two tracks not satisfying the energy requirements are selected, and the correction is estimated by fitting the two-dimensional $\mathrm{d}E/\mathrm{d}x$ distribution of the two tracks in these events with a model containing three components: Bhabha events, di-muon events, and a background of uniform distribution. The uncertainty is estimated as the difference in result between the two correction methods.

The uncertainty on the predictions of the BABAYAGA@NLO generator is assigned to be 0.1%, following Ref. [9].

The total uncertainty for each energy point is summarized in Table III. The uncertainties from different sources are assumed to be independent, therefore the total uncertainties are obtained by adding up the uncertainties in quadrature.

TABLE III. The relative systematic uncertainties (in %) for the integrated luminosities of the new XYZ data set.

Sample (MeV)	4190	4200	4210	4220	4237	4246	4270	4280
Tracking efficiency	0.13	0.17	0.05	0.08	0.24	0.15	0.30	0.29
Requirement on energy	0.12	0.11	0.12	0.14	0.09	0.12	0.13	0.10
Requirement on $\cos\theta$	0.24	0.22	0.21	0.22	0.32	0.37	0.43	0.39
Requirement on momentum	0.14	0.08	0.01	0.00	0.17	0.06	0.09	0.01
CM energy	0.06	0.07	0.00	0.01	0.04	0.04	0.02	0.01
MC sample size	0.2	0.2	0.2	0.2	0.2	0.2	0.2	0.2
Correction of EMC readout error	0.05	0.06	0.08	0.04	0.07	0.06	0.06	0.05
Event generator	0.1	0.1	0.1	0.1	0.1	0.1	0.1	0.1
Total	0.41	0.39	0.35	0.35	0.45	0.50	0.59	0.55

VI. UPDATE ON THE LUMINOSITY OF THE 2010–2014 DATA SETS

An update of the integrated luminosities for the 21 data samples collected in 2010-2014, previously reported in Ref. [5], is needed in order to apply the EMC readout correction, as described in the previous section, and to include additional events coming from the recovery of data files that were not originally available.

The same procedure described for the 2016-2017 data samples has been applied for this update, with the same configurations of the MC generator, the same event selection criteria, and the same EMC readout correction. The BABAYAGA@NLO event generator we use in this analysis has a significantly better precision than the event generator used in the previous analysis [5] (0.1% versus 0.5%), which contributes to the reduction of the total uncertainties.

Table IV summarizes the updated integrated luminosities with statistical uncertainties, the correction factors due to the EMC readout error, and the comparison with the results of the previous analysis. The results of the three lowest energy points (samples 3810, 3900, and 4009) are not updated, since there is no file update and, according to the correlation between the amount of the EMC readout correction and the CM energies in other data sets, the EMC readout correction is

expected to be negligible at these energy points. We skip the unnecessary update of these data samples to avoid dealing with the computational difficulty of the MC sampling over narrow resonances. For the remainder of the energy points, the updated results are $0.3\% - 4.8\%$ larger than the original values. The discrepancies are mainly caused by the EMC readout correction, and for a few data sets such as 4420_1 and 4600 there're also the contributions from recovery of data files. Figure 4 shows the correlation between the sizes of the EMC readout correction and the CM energies. This figure shows that the size of this correction grows exponentially as the CM energy increases, indicating that the problem may grow to be much more severe if BESIII is to operate in higher energy zones. Besides, the fact that the frequencies of EMC readout error fit well to an exponential model may hint at its mechanism.

TABLE IV. The updated integrated luminosities of the 2010–2014 XYZ data sets, the correction factor due to the EMC readout error ($\sigma_{\rm EMC} = {\rm N_{cor}}/{\rm N_{obs}}$), and comparison with the previous results [5]. The first uncertainties are statistical and the second ones are systematic.

$E_{\rm cm}({\rm MeV})$	$\sigma_{\rm EMC}$ (%)	Updated $\mathcal{L}$ (pb^{-1})	Previous $\mathcal{L}$ (pb^{-1})	Difference (%)
3810	-	-	50.54 ± 0.03	-
3900	-	-	$52.61 \pm 0.03 \pm 0.51$	-
4009	-	-	$482.0 \pm 0.1 \pm 4.7$	-
4090	0.07 ± 0.04	$52.86 \pm 0.03 \pm 0.35$	$52.63 \pm 0.03 \pm 0.51$	$+0.43$
4190	0.19 ± 0.04	$43.33 \pm 0.03 \pm 0.29$	$43.09 \pm 0.03 \pm 0.42$	$+0.56$
4210	0.24 ± 0.00	$54.95 \pm 0.03 \pm 0.36$	$54.55 \pm 0.03 \pm 0.53$	$+0.73$
4220	0.24 ± 0.04	$54.60 \pm 0.03 \pm 0.36$	$54.13 \pm 0.03 \pm 0.53$	$+0.86$
4230_1	0.27 ± 0.04	$44.54 \pm 0.03 \pm 0.29$	$44.40 \pm 0.03 \pm 0.43$	$+0.32$
4230_2	0.27 ± 0.04	$1056.4 \pm 0.1 \pm 7.0$	$1047.3 \pm 0.1 \pm 10.1$	$+0.86$
4245	0.31 ± 0.03	$55.88 \pm 0.03 \pm 0.37$	$55.59 \pm 0.04 \pm 0.54$	$+0.53$
$4260_{1,2}$	0.34 ± 0.04	$828.4 \pm 0.1 \pm 5.5$	$523.7 \pm 0.1 \pm 5.1$	$+0.32$
			$302.0 \pm 0.1 \pm 3.0$	
4310	0.51 ± 0.06	$45.08 \pm 0.03 \pm 0.30$	$44.90 \pm 0.03 \pm 0.44$	$+0.40$
4360	0.74 ± 0.06	$544.0 \pm 0.1 \pm 3.6$	$540.0 \pm 0.1 \pm 5.2$	$+0.76$
4390	0.95 ± 0.05	$55.57 \pm 0.04 \pm 0.37$	$55.18 \pm 0.04 \pm 0.54$	$+0.70$
4420_1	1.13 ± 0.07	$46.80 \pm 0.03 \pm 0.31$	$44.67 \pm 0.03 \pm 0.43$	$+4.77$
4420_2	1.20 ± 0.06	$1043.9 \pm 0.1 \pm 6.9$	$1028.9 \pm 0.1 \pm 10.0$	$+1.45$
4470	1.71 ± 0.03	$111.09 \pm 0.04 \pm 0.73$	$109.94 \pm 0.04 \pm 1.07$	$+1.05$
4530	2.38 ± 0.11	$112.12 \pm 0.04 \pm 0.73$	$109.98 \pm 0.04 \pm 1.07$	$+1.95$
4575	3.13 ± 0.14	$48.93 \pm 0.03 \pm 0.32$	$47.67 \pm 0.03 \pm 0.46$	$+2.64$
4600	3.51 ± 0.15	$586.9 \pm 0.1 \pm 3.9$	$566.9 \pm 0.1 \pm 5.5$	$+3.52$

Systematic uncertainties are assigned following the same procedure as for the 2016–2017 data sets. For each source of uncertainty, we take the maximum uncertainty for all the energy points. These uncertainties from individual sources are then added up in quadrature to obtain the total systematic uncertainty. The result is summarized in Table V. The total systematic uncertainty is determined to be 0.66% for all the energy points except for the lowest three energy points, for which we quote the original uncertainty 0.97% [5].

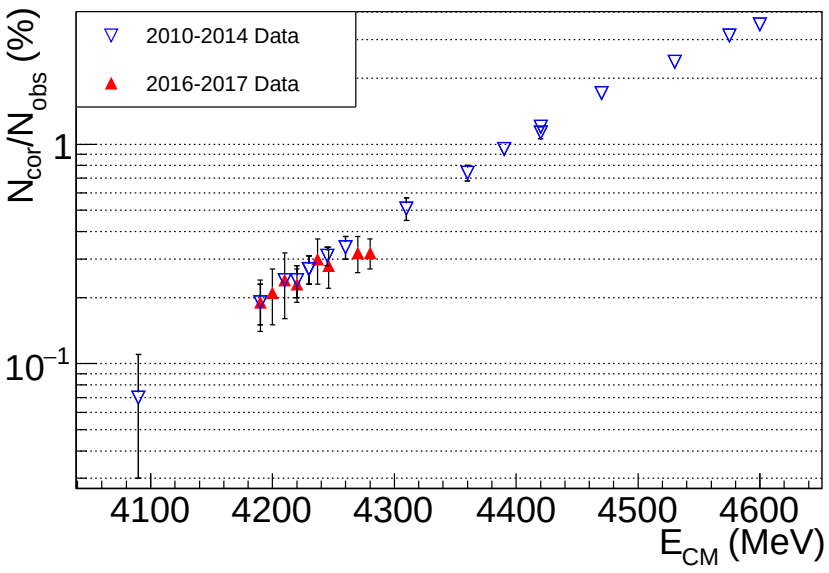

FIG. 4. The logarithm of relative sizes of the EMC readout correction at different CM energies for 2010-2014 (blue) and 2016-2017 (red) XYZ data sets. In this plot, the data points have a seemingly linear relationship, suggesting that the frequencies of the EMC readout errors may grow exponentially as the CM energy further increases.

TABLE V. The systematic uncertainties of the integrated luminosities of the 2010–2014 XYZ data samples, excluding those at the lowest three energy points. For each source of uncertainty, the maximum value across all the energy points is taken as the overall estimation.

Source	Relative uncertainty (%)
Tracking efficiency	0.42
Requirement on energy	0.28
Requirement on $\cos\theta$	0.14
Requirement on momentum	0.29
CM energy	0.07
MC sample size	0.20
Correction of EMC readout errors	0.15
Event generator	0.10
Total	0.66

VII. SUMMARY

We have measured the integrated luminosities of the XYZ data sets taken at BESIII from 2016 to 2017, and the results are listed in Table I. Additionally, we have updated the luminosity measurement of the XYZ data taken from 2010 to 2014, with corrections arising from an improved understanding of the EMC performance and the recovery of data files, as shown in Table IV. These high precision results are of fundamental importance for the measurements of the production cross sections of the XYZ particles as well as those of conventional charmonium states in this energy

range, which will enable a more precise comparison with the predictions of the quark model and an improved understanding of QCD. The results presented in this work have been used in several recent analyses of the BESIII collaboration (e.g. see Refs. [11–13]) and will be used by many other analyses in the future.

Figure 4 shows that the impact of the EMC readout errors may grow exponentially to above 10% as the CM energy increases to around 5.0 GeV. This means that the dangerous effect warrants more inspection if BESIII is to operate in higher energy zones with BEPCII update project in the future.

VIII. ACKNOWLEDGEMENT

The BESIII collaboration thanks the staff of BEPCII and the IHEP computing center for their strong support. This work is supported in part by National Key R&D Program of China under Contracts Nos. 2020YFA0406300, 2020YFA0406400; National Natural Science Foundation of China (NSFC) under Contracts Nos. 11625523, 11635010, 11735014, 11822506, 11835012, 11935015, 11935016, 11935018, 11961141012, 12022510, 12025502, 12035009, 12035013, 12061131003; the Chinese Academy of Sciences (CAS) Large-Scale Scientific Facility Program; Joint Large-Scale Scientific Facility Funds of the NSFC and CAS under Contracts Nos. U1732263, U1832207; CAS Key Research Program of Frontier Sciences under Contract No. QYZDJ-SSW-SLH040; 100 Talents Program of CAS; INPAC and Shanghai Key Laboratory for Particle Physics and Cosmology; ERC under Contract No. 758462; European Union Horizon 2020 research and innovation programme under Contract No. Marie Sklodowska-Curie grant agreement No 894790; German Research Foundation DFG under Contracts Nos. 443159800, Collaborative Research Center CRC 1044, GRK 2149; Istituto Nazionale di Fisica Nucleare, Italy; Ministry of Development of Turkey under Contract No. DPT2006K-120470; National Science and Technology fund; Olle Engkvist Foundation under Contract No. 200-0605; STFC (United Kingdom); The Knut and Alice Wallenberg Foundation (Sweden) under Contract No. 2016.0157; The Royal Society, UK under Contracts Nos. DH140054, DH160214; The Swedish Research Council; U. S. Department of Energy under Contracts Nos. DE-FG02-05ER41374, DE-SC-0012069.

[1] M. Ablikim *et al.* [BESIII Collaboration], Nucl. Instrum. Meth. A **614**, 345 (2010).

[2] Q. Qin, L. Ma, J. Wang and C. Zhang, Conf. Proc. C **100523**, WEXMH01 (2010) IPAC-2010-WEXMH01.

[3] M. Ablikim *et al.*, Chin. Phys. C **44**, 040001 (2020).

[4] For recent reviews, see N. Brambilla, S. Eidelman, C. Hanhart, A. Nefediev, C. P. Shen, C. E. Thomas, A. Vairo and C. Z. Yuan, Phys. Rept. **873**, 1 (2020); F. K. Guo, C. Hanhart, U. G. Meißner, Q. Wang, Q. Zhao and B. S. Zou, Rev. Mod. Phys. **90**, 015004 (2018); H. X. Chen, W. Chen, X. Liu and S. L. Zhu, Phys. Rept. **639**, 1 (2016); N. Brambilla *et al.*, Eur. Phys. J. C **71**, 1534 (2011).

[5] M. Ablikim *et al.* [BESIII Collaboration], Chin. Phys. C **39**, 093001 (2015).

[6] X. Li *et al.*, Radiat. Detect. Technol. Methods **1**, 13 (2017); Y. X. Guo *et al.*, Radiat. Detect. Technol. Methods **1**, 15 (2017); P. Cao *et al.*, Nucl. Instrum. Meth. A **953**, 163053 (2020).

[7] J. Allison *et al.*, IEEE Trans. Nucl. Sci. **53**, 270 (2006).

[8] M. Ablikim *et al.* [BESIII Collaboration], Chin. Phys. C **45**, 103001 (2021).

[9] G. Balossini *et al.*, Phys. Lett. B **663**, 209 (2008).
[10] C.H. Yu, Z. Duan, S. Gu, Y.Y. Guo, X.Y. Huang, D. Ji, *et al.*, "BEPCII Performance and Beam Dynamics Studies on Luminosity", in *Proc. 7th Int. Particle Accelerator Conf. (IPAC'16)*, Busan, Korea, May 2016, paper TUYA01, pp. 1014–1018,
[11] M. Ablikim *et al.* [BESIII Collaboration], Phys. Rev. Lett. **122**, 232002 (2019).
[12] M. Ablikim *et al.* [BESIII Collaboration], Phys. Rev. Lett. **122**, 202001 (2019).
[13] M. Ablikim *et al.* [BESIII Collaboration], Phys. Rev. D **103**, 052003 (2021).